Available online at www.sciencedirect.com
ScienceDirect
Journal of Molecular Graphics and Modelling 26 (2007) 709–719
Journal of Molecular Graphics and Modelling
www.elsevier.com/locate/JMGM

Biochemical characterization, homology modeling and docking studies of ornithine δ-aminotransferase—an important enzyme in proline biosynthesis of plants

P. Nataraj Sekhar [a], R. Naga Amrutha [a], Shubhada Sangam [a], D.P.S. Verma [b], P.B. Kavi Kishor [a,*]

[a] *Department of Genetics, Osmania University, Hyderabad 500007, India*
[b] *Center for Biotechnology, Ohio State University, Columbus, OH 43210, USA*

Received 18 November 2006; received in revised form 27 April 2007; accepted 28 April 2007
Available online 3 May 2007

Abstract

Ornithine δ-aminotransferase (OAT) is an important enzyme in proline biosynthetic pathway and is implicated in salt tolerance in higher plants. OAT transaminates ornithine to pyrroline 5-carboxylate, which is further catalyzed to proline by pyrroline 5-carboxylate reductase. The *Vigna aconitifolia* OAT cDNA, encoding a polypeptide of 48.1 kDa, was expressed in *Escherichia coli* and the enzyme was partially characterized following its purification using $(NH_4)_2SO_4$ precipitation and gel filtration techniques. Optimal activity of the enzyme was observed at a temperature of 25 °C and pH 8.0. The enzyme appeared to be a monomer and exhibited high activity at 4 mM ornithine. Proline did not show any apparent effect but isoleucine, valine and serine inhibited the activity when added into the assay mixture along with ornithine. Omission of pyridoxal 5′-phosphate from the reaction mixture reduced the activity of this enzyme by 60%. To further evaluate these biochemical observations, homology modeling of the OAT was performed based on the crystal structure of the ornithine δ-aminotransferase from humans (PDB code 1OAT) by using the software MODELLER6v2. With the aid of the molecular mechanics and dynamics methods, the final model was obtained and assessed subsequently by PROCHECK and VERIFY-3D graph. With this model, a flexible docking study with the substrate and inhibitors was performed and the results indicated that Gly106 and Lys256 in OAT are the important determinant residues in binding as they have strong hydrogen bonding contacts with the substrate and inhibitors. These observations are in conformity with the results obtained from experimental investigations.

Keywords: Docking; GOLD; Homology modeling; Ornithine δ-aminotransferase; Proline biosynthesis; Salt tolerance

1. Introduction

Proline plays an important role in the adaptation of plant cells to drought and salinity stresses [6]. In *Escherichia coli*, glutamate is converted to proline via the intermediates γ-glutamyl phosphate, GSA and P5C [5,12]. However, in plants, glutamate gets converted to P5C directly by P5C synthetase and then to proline by P5C reductase. The formation of proline from ornithine proceeds either via α- or δ-transamination of ornithine to P2C in prokaryotes or P5C in eukaryotes respectively, followed by reduction. Much of the evidence from both plant and animal studies suggest the occurrence of the latter pathway [28,7]. OAT, a pyridoxal 5′-phosphate (PLP) dependent and a mitochondrial located enzyme, catalyzes the transfer of the δ-amino group of L-ornithine to 2-oxoglutarate, producing L-glutamyl γ-semialdehyde, which spontaneously cyclizes to pyrroline 5-carboxylate. The operation of both glutamate and ornithine pathways was demonstrated in plants. In *Vigna aconitifolia* (mothbean), salt stress and nitrogen starvation upregulated P5CS but down-regulated the mRNA levels of OAT. On the other hand, mRNA levels of OAT increased in plants supplied with excess nitrogen.

Abbreviations: BLAST, basic local alignment search tool; cDNA, complementary DNA; GOLD, genetic optimization for ligand docking; GSA, glutamic γ-semialdehyde; NCBI, national center for biotechnology information; OAT, ornithine δ-aminotransferase; PLP, pyridoxal-5′-phosphate; pdfs, probability density functions; PDB, protein databank; P5C, Δ^1-pyrroline 5-carboxylate; P2C, pyrroline 2-carboxylate; P5CS, Δ^1-pyrroline 5-carboxylate synthetase; RMS, root mean-square; RMSD, root mean square deviation; SCRs, structurally conserved regions; SVRs, structurally variable regions

* Corresponding author. Tel.: +91 40 2768 2335; fax: +91 40 2709 5178.
E-mail address: pbkavi@yahoo.com (P.B.K. Kishor).

1093-3263/$ – see front matter © 2007 Elsevier Inc. All rights reserved.
doi:10.1016/j.jmgm.2007.04.006

These results indicated clearly that glutamate pathway is predominant for proline synthesis during salt stress. But, ornithine pathway is upregulated when plants are supplied with high nitrogen [7]. However, it is not known whether glutamate or ornithine pathway predominates in humans for proline biosynthesis. Hyperornithemia in humans arise due to dysfunction of OAT and ultimately leads to gyrate atrophy, a recessive genetic disease, which leads to progressive loss of vision and eventually blindness in humans [26]. Crystallization and preliminary X-ray diffraction studies of recombinant human ornithine aminotransferase and the crystal structure of it were determined by Shen et al. [27]. The crystals of this enzyme belong to the trigonal space $P3_121$ with unit cell parameters $a = b = 116.3$ Å and $c = 190.0$ Å, $\alpha = \beta = 90^\circ$, $\gamma = 120^\circ$. Studies in humans revealed that there are three monomers per asymmetric unit of OAT [27]. However, there is no report yet available on the purification and also on the crystal structure of OAT in plants. We therefore, propose in this communication a stereo chemically feasible model for the three-dimensional structure of a plant OAT and report its biochemical characterization as well.

2. Materials and methods

2.1. Preparation of enzyme extract and partial purification

E. coli DH5α cells containing the plasmid pVOT1 (obtained from Dr. D.P.S. Verma, USA) were grown in a liquid Luria and Bertaini medium [18] at 37 °C for 12–14 h. Bacterial cells harbouring plant OAT were harvested by centrifugation at 3000 × *g*. The cells were then suspended in 10 ml of 50 mM phosphate buffer (pH 8.0), containing 1 mM dithiothreitol at 4 °C and sonicated at 50 W (Benson Sonifier type 450, USA). The slurry was centrifuged at 16,000 × *g* for 20 min at 4 °C. The supernatant was fractionated by $(NH_4)SO_4$ precipitation at 5 °C. Enzyme fraction precipitating between 40 and 60% saturation of $(NH_4)SO_4$ was dissolved in 50 mM phosphate buffer (pH 8.0), dialyzed and subjected to gel filtration chromatography on a Superose-6-high performance liquid chromatography column. The partially purified enzyme was used for assaying the specific activity of OAT.

2.2. Kinetic studies of OAT

The mothbean OAT enzyme was expressed in *E. coli* DH5α cells and the enzyme was partially purified as described. The reaction optimum for pH, temperature, substrate concentration, α-ketoglutarate and the cofactor pyridoxal 5′-phosphate (PLP) were determined. Amino acids such as proline, isoleucine, valine and serine were added separately (all at a concentration of 1 mM each) in the assay mixture along with the substrate ornithine and their effect on OAT activity was examined.

2.3. Assay of OAT

The activity of OAT was determined in a reaction mixture containing 3 μmol of ornithine, 3 μmol of α-keto-glutarate, 1 μmol of $MgCl_2$, 1 μmol of PLP and a suitable aliquot of the enzyme in 50 mM phosphate buffer (pH 8.0). The reaction was carried out at 25 °C and terminated by adding 0.5 ml of *ortho*-aminobenzaldehyde (Sigma, USA). The reaction mixture was incubated for 5 min in a boiling water bath, the precipitate was centrifuged and the optical density of the supernatant containing the product P5C was measured at 440 nm. The product concentration was estimated from a standard curve prepared with an authentic sample of P5C. Protein concentration in the cell extract was determined from a standard curve prepared with bovine serum albumin following the method of Bradford [4]. Specific activity of OAT is expressed as μg of P5C formed min^{-1} mg^{-1} protein.

2.4. 3D model building

The initial model of *Vigna* OAT was built by using homology-modeling methods and MODELLER6v2 software on IRIX environment using silicon graphics O^{2+} machine. This program is used for comparative protein structure modeling that optimally satisfies spatial restraints derived from the alignment and expressed as probability density functions (pdfs) for the features restrained. The pdfs restrain Cα–Cα distances, main-chain N–O distances, main-chain and side-chain dihedral angles. The 3D model of the protein is obtained by optimization of the molecular pdf such that the model violates the input restraints as little as possible. The molecular pdf is derived as a combination of pdfs restraining individual spatial features of the whole molecule. The optimization procedure is a variable target function method that applies the conjugate gradients algorithm to positions of all non-hydrogen atoms [25]. The sequence of the OAT enzyme (Accession Number: P31893) was obtained from NCBI database [6]. The query sequence from *Vigna* was searched to find out the related protein structure to be used as a template by the BLAST program [2,3] against PDB. Sequences were aligned and the one that showed the maximum identity with high score and less *e*-value was used as a reference structure to build a 3D model for OAT. The coordinates for the SCRs for OAT were assigned from the template using multiple sequence alignment, based on the Needleman–Wunsch algorithm [20,31]. The structure having the least modeller objective function, obtained from the modeller was improved by energy minimization. Initial geometric optimizations were carried out using the standard Tripos force field with 0.05 kcal/mol energy convergence criteria and a distant-dependent dielectric constant of 4.0 *R* to take into account the dielectric shielding in proteins employing Gasteiger–Marsili charges (SYBYL 6.7, Tripos Inc., MO, USA) with non-bonding interaction cut off as 15. All hydrogen atoms were included during the calculation. After undertaking 100 steps of Powell minimization method initially [21,22], a conjugate gradient energy minimization of the full protein was carried out until the RMS gradient was lower than 0.05 kcal/mol. To examine the quality of the model structures and their stability, 1000 femto seconds (fs) simulations at an ensemble of constant number of particles, volume, and temperature of 300 K were performed. Boltzmann initial velocities and random number seed with a tolerance of 0.0001

were used for the above calculations. The same force field setup as that for energy minimization was used. Snapshots were taken every 5 fs with a coupling phase of 100 fs. Parameters were set to mimic the solvation effect [1]. Finally, the average structure was again subjected to energy minimization methods as described above. All calculations were performed on the SGI 2000 workstation using the SYBYL software suite operating under IRIX (SYBYL 6.7, Tripos Inc., MO, USA). In this step, the quality of the initial model was improved. The final structure obtained was analyzed by Ramachandran's map using PROCHECK, a program used to check the stereo chemical quality of protein structures [16] and environment profile using VERIFY-3D (a structure evaluation server) graph [17]. This model was used to identify the active site and for docking of the substrate with the enzyme.

2.5. Active site identification of OAT enzyme

The active site of OAT from *Vigna* was identified using SiteID of SYBYL software suite. This method generated many possible spheres of the radius of water inside the protein molecules in search of the largest space or cluster available, which could be identified as an active site. A flood fill algorithm, similar to the one implemented in CAVITY was used [11]. For each solvent molecule in the pocket, all atoms in the protein lying within a specific distance of 5 Å are considered. The unions of all such atoms are considered as belonging to the active site. Besides, electrostatic or polar surface identification method was used to distinguish between the actual site and the other smaller cluster of sites.

2.6. Docking studies

The ligands, including all hydrogen atoms, were built and minimized with SYBYL software suite as described above. GOLD version 2.1.2 (Cambridge Crystallographic Data Center, Cambridge, United Kingdom) was used for docking OAT enzyme for 50 times [14]. The active site was defined as the collection of protein residues enclosed within a 15 Å radius sphere. The annealing parameters for van der Walls and hydrogen bonding were set to 4.0 and 2.5 Å, respectively. The parameters used for genetic algorithm were population size (100), selection pressure (1.1), number of operations (1,00,000), number of islands (5), niche size (2), migrate (10), mutate (95) and cross-over (95). The default speed selection was used to avoid a potential reduction in docking accuracy. Fifty genetic algorithm runs with default parameter settings were performed without early termination. To estimate the protein–ligand complexes, the scoring function GOLD score was employed [14].

Table 1
Effect of amino acids on the specific activity of recombinant OAT activity[a]

Substrate + amino acid	Specific activity (μg of P5C formed min^{-1} mg^{-1} protein)
Ornithine (control)	34.6 (±7.2)
Ornithine + isoleucine	2.9 (±8.1)
Ornithine + valine	5.3 (±2.0)
Ornithine + serine	10.8 (±3.4)
Ornithine + proline	33.8 (±6.9)

[a] Amino acids were added to the assay mixture along with the substrate ornithine. Data represent an average of six replicates.

3. Results

3.1. Biochemical characterization of OAT enzyme

The cDNA clone of moth bean OAT is 1559 base pair long and contained a single open reading frame that encoded a polypeptide of 48.1 kDa. The gene was expressed in *E. coli* and the enzyme OAT was extracted from bacterial cells by sonication and partially purified using ammonium sulphate precipitation. The fraction precipitating between 40 and 60% saturation of $(NH_4)SO_4$ was used for enzyme assay. The $(NH_4)SO_4$ precipitate was dissolved in 50 mM phosphate buffer pH 8.0, dialyzed, and subjected to gel filtration. Gel filtration was carried out on a Superose-6-high performance liquid chromatography column. Specific activity of recombinant protein OAT was determined using ornithine as a substrate and also by adding other amino acids into the assay mixture individually along with the substrate (Table 1). The assay was carried out at 25 °C and at pH 8.0 (found as optimum). The K_m values for ornithine and α-ketoglutarate were found as 2 and 0.75 mM, respectively. Proline did not affect the enzyme but isoleucine, valine and serine inhibited the activity significantly (Table 1). Omission of PLP from the reaction mixture reduced the specific activity of the enzyme to 13.5 compared to 34.6 in presence of it (60% reduction).

3.2. Homology modeling of OAT enzyme

In the results of BLAST search against PDB, only four-reference proteins, including ornithine δ-aminotransferase (1OAT) from human [27], ornithine δ-aminotransferase (2OAT) complexed with 5-fluoromethylornithine [29], human ornithine complexed with L-canaline (2CAN) [26] and human

Table 2
Data for the closest homologue with known 3D structures obtained with the BLAST server against PDB

PDB	Protein	Chain	Authors	Identity to OAT (%)
1OAT	Crystal structure of Human recombinant ornithine aminotransferase	A, B, C	Shen et al. (1997)	64
2OAT	Ornithine aminotransferase complexed with 5-Fluoromethylornithine	A, B, C	Storici et al. (1999)	64
2CAN	Human ornithine aminotransferase complexed with L-canaline	A, B, C	Shah et al. (1997)	64
1GBN	Human ornithine aminotransferase complexed with the neurotoxin gabaculine	A, B, C	Shah et al. (1997)	64

CLUSTAL W (1.82) multiple sequence alignment

```
1oat       ----GPPTSDDIFEREYKYGAHNYHPLPVALERGKGIYLWDVEGRKYFDFLSSYSAVNQGHC
OAT        GLKS-----VTSEQVFEREQKYGAHNYHHCSAYRAKGVSLDMEGKRYFDFLSAYSAVNQGHC
                 **:::**** ********    :  *.**: * *:**::******:*********

1oat           HPKIVNALKSQVDKLTLTSRAFYNNVLGEYEEYITKLFNYHKVLPMNTGVEAGETACKLA
OAT            HPKIVNTMVEQAQRLTLTSRAFYTDVLGEYEEFLTKLFNYDKVLPMNTGVEGGETACKIA
               ******:: .*.::*********.:*******::******.**********.******:*

1oat           RKWGYTVKGIQKYKAKIVFAAGNFWGRTLSAISSSTDPTSYDGFGPFMPGFDIIPYNDLP
OAT            RCWAYMKKKVPENQAKIIFAENNFWGRTLSAISASTDPMSYDELRPYMPGFEIVKYNDTA
                 * *.*  * : : :***:** .***********:**** *** : *:****:*: *** .

1oat           ALERALQDPNVAAFMVEPIQGEAGVVVPDPGYLMGVRELCTRHQVLFIADEIQTGLARTG
OAT            ALEKAFQDPNVCAYMVEPIQGEAGVVALDAGYLTEVRELCTKYNVLFIADEVQTGLARTG
               ***:*:*****.*:************. *.***  ******:::*******:********

1oat           RWLAVDYENVRPDIVLLGKALSGGLYPVSAVLCDDDIMLTIKPGEHGSTYGGNPLGCRVA
OAT            RMLAVDHEDVKPDLLILGKALSGGLYPVSAVLRDDHIMDCIQPGLHTAMDVMDPRMRILA
               * ****:*:*:**:::**************** **.**  *:** * :    :*    :*

1oat           IAALEVLEEENLAENADKLGIILRNELMKLPSDVVTAVRGKGLLNAIVIKETKDWDAWKV
OAT            ASRYYVRVARERCENAQIQATYLRKELNTLPKDVVPVVRGKGLLNAIVIN--KKFDAWDV
                :   *   .: .***:  .  **:** .**.***..************:  *.:***.*

1oat           CLRLRDNGLLAKPTHGDIIRFAPPLVIKEDELRESIEIINKTILSF
OAT            CLN------LCKPTHGDIIRFATTGHHRGTDPRMCQYYQKYH----
               **.      *.***********..   :  : * .    :
```

Fig. 1. Sequence alignment of OAT from *Vigna aconitifolia* with ornithine aminotransferase (PDB code 1OAT) carried out using CLUSTALW server that was subsequently submitted to MODELLER. The conserved regions are indicated by '*'.

ornithine δ-aminotransferase complexed with the neurotoxin gabaculine (1GBN) [26], exhibited a high level of sequence identity. The amino acid sequence identity of these reference proteins with the OAT was 64, 64, 64 and 64%, respectively (Table 2). Structurally conserved regions (SCRs) for the model and the template were determined by superimposition of the two structures and pair wise alignment (Fig. 1). In the subsequent studies, 1OAT was chosen as a reference structure for modeling *Vigna* OAT. Coordinates from the reference protein (1OAT) to the SCRs, SVRs, N-termini and C-termini were assigned to the target sequence based on the satisfaction of spatial restraints. All side chains of the model protein were set by rotamers. The initial model was thus generated with the above procedure and subsequently possible active sites were searched using SYBYL SiteID module and the results were compared with the active site of 1OAT. Thus, care was taken that residues 1–35 did not locate near the active site. In this study, residues 1–35 were removed from the model because no homologous region occurred in 1OAT and these residues did not locate near the active site. Therefore, the present model is made up of residues 36–426. The options used for running the MODELER6v2 are shown in Table 3. But the model was refined by molecular dynamics method and the final stable structure of the OAT enzyme obtained is shown in Fig. 2. It is evident from the Fig. 2 that this enzyme contains 15 helices and 13 sheets. The final structure was subsequently checked by VERIFY-3D graph and the results are shown in Fig. 3. The compatibility score above zero in the VERIFY-3D graph (Fig. 3) corresponded to acceptable side chain environments.

Table 3
Options used in MODELLER program

INCLUDE # Include the predefined TOP routines	
SET ALNFILE	= 'alignment1'
SET KNOWNS	= '1OAT'
SET SEQUENCE	= 'query'
SET HETATM_IO	= on
SET WATR_IO	= off
SET HYDROGEN	= off
SET STARTING_MODEL	= 1
SET ENDING_MODEL	= 20
CALL ROUTINE	= 'model'

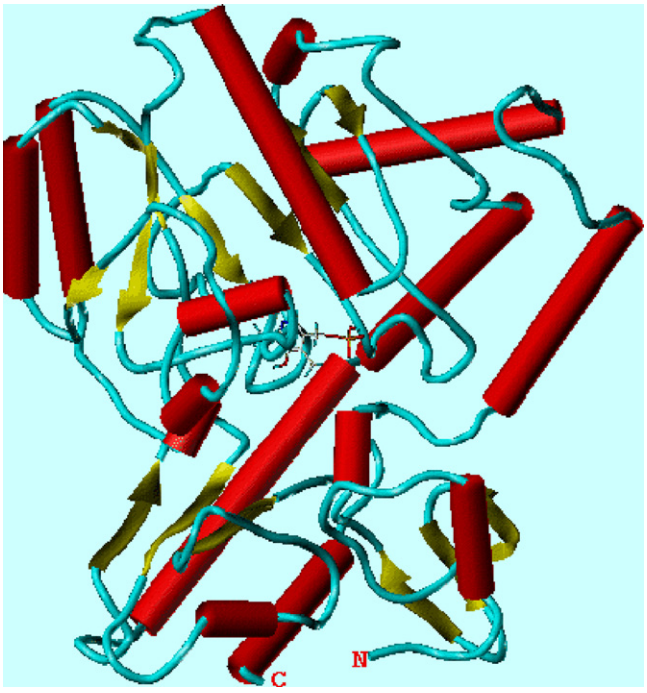

Fig. 2. The final 3D structure of OAT enzyme is obtained by minimizing the energy of the average conformation over the last 1000 fs of molecular dynamics simulation. Red colour cylinders represent α-helix and yellow arrows represent β-sheets. N and C terminals are represented in red colour.

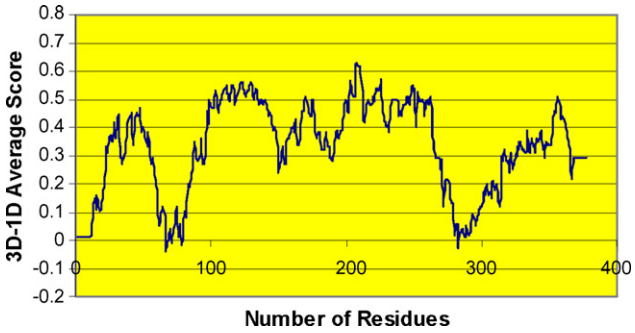

Fig. 3. The 3D profiles verified results of OAT model, where residues with positive compatibility score are reasonably folded.

All residues appeared to be reasonable from Fig. 4 and therefore it is believed that the structure of OAT is reliable.

3.3. Validation of OAT enzyme

Validation of the model was carried out using Ramachandran's plot calculations computed with PROCHECK program. The ϕ and φ distributions of the Ramachandran's plot of non-glycine, non-proline residues are summarized in Fig. 4 and Table 4. The RMSD for covalent bonds relative to the standard dictionary was −0.21 Å and for the covalent angles was −0.48°. Altogether, 98.4% of the residues was in favored and allowed regions. The overall PROCHECK G-factor was −0.08 and VERIFY-3D environment profile was found to be good.

Table 4
Ramachandran plot calculations on 3D model of OAT computed with the PROCHECK program

% of residue in most favored regions	75.1
% of residue in the additionally allowed zones	23.2
% of residue in the generously regions	0.3
% of residue in disallowed regions	1.4
% of non-glycine and non-proline residues	100.0

3.4. Superimposition of template with OAT enzyme

The structural superimposition of Cα trace of template and OAT enzyme is shown in Fig. 7. The weighted RMSD of Cα trace between 1OAT and OAT was 2.0 Å with an identity score of 63.2 and significance score of 46% and the weighted RMSD of Cα trace between 2OAT and OAT was 2.0 Å with a significance score of 46%. This further indicated that the homology model is reliable. Hence, this model was used for the identification of active site and for docking the inhibitors with the enzyme.

3.5. Secondary structure prediction

Amino acid sequences of template and final OAT were aligned using CLUSTALW. The secondary structures were also analyzed and compared by the JOY [19] program (protein sequence-structure representation and analysis). It was found that the secondary structures of template and final OAT are

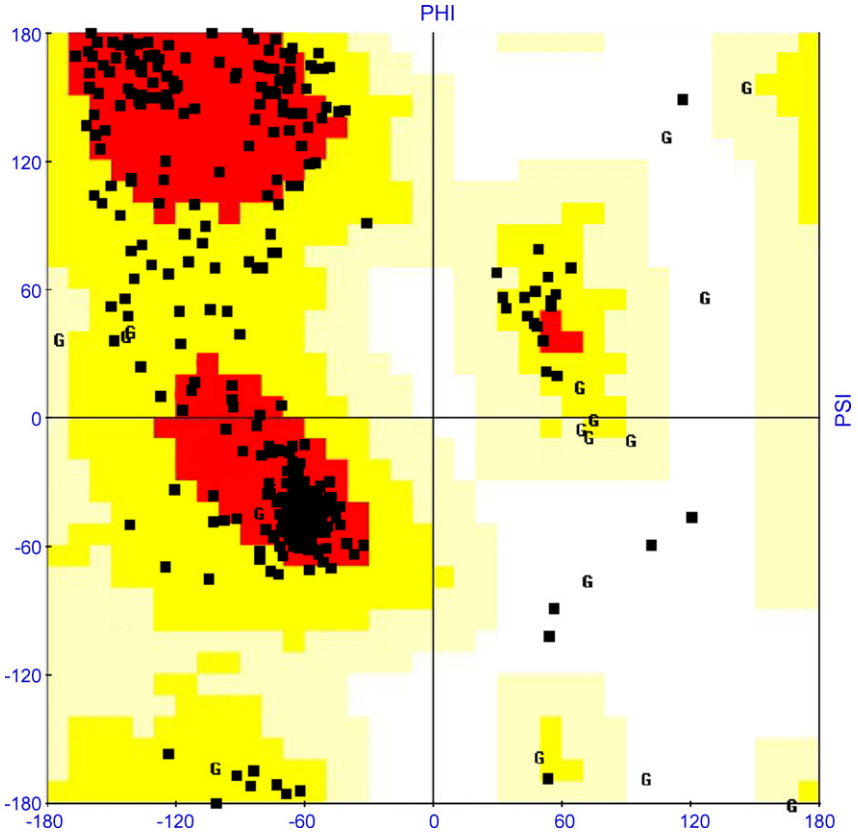

Fig. 4. Ramachandran's map of OAT enzyme. The map was built using MODELLER6v2 software. The plot calculations on 3D model of OAT enzyme was computed with the PROCHECK program.

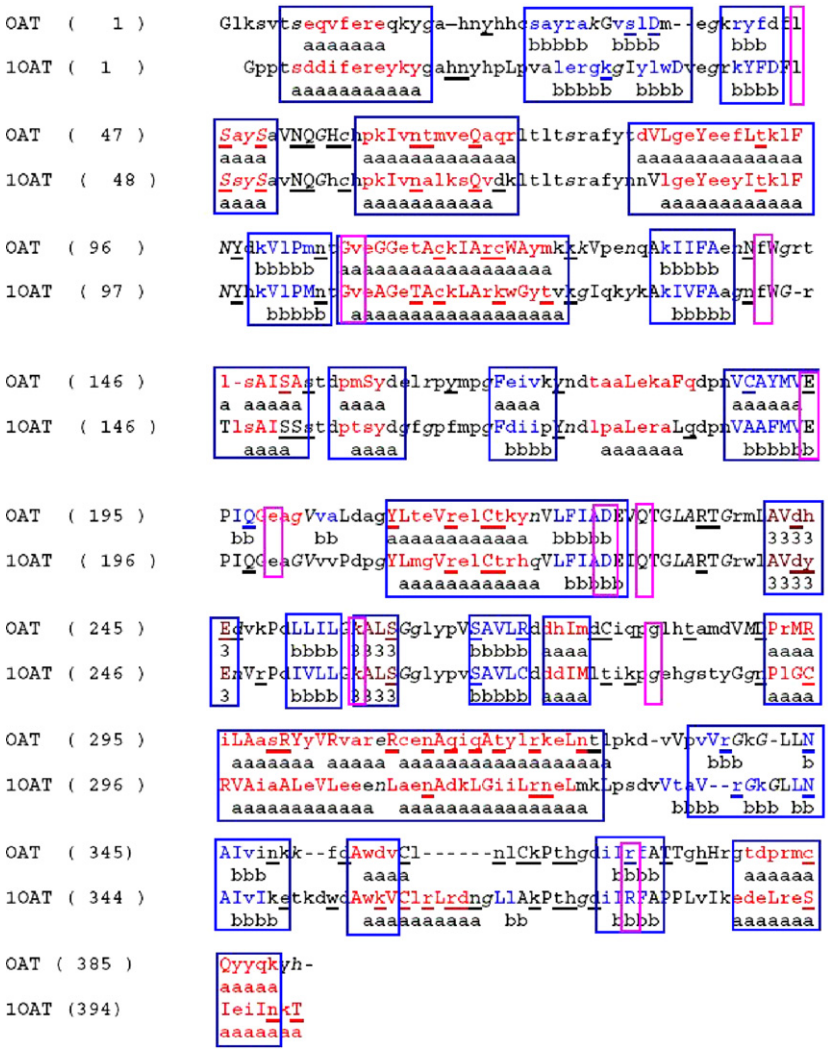

Fig. 5. Structure–structure alignment of template, and the final structure of OAT enzyme built using JOY program. Boxes coloured with red indicate conserved secondary structures and with pink indicate conserved active site residues for substrate binding. Key to the JOY alignment for HTML output is given as under:

Solvent inaccessible	Upper case	X
Solvent accessible	Lower case	x
Alpha helix	Red	x
Beta strand	Blue	x
3–10 helix	Maroon	x
Hydrogen bond to main chain amide	Bold	x
Hydrogen bond to main chain carbonyl	Underline	x
Positive phi	Italic	*x*

Tilde and Breve are not displayed in the HTML output. Colours are only for colour PostScript and HTML outputs.

highly conserved as shown in Fig. 5 and this structure was subsequently used for active site identification.

3.6. Active site identification of OAT enzyme

After the final model was built, the binding sites of OAT were searched using the SiteID module which revealed 12 possible sites (Fig. 6). These pockets were compared with the active site of the template and was found that site 4 (violet region in Fig. 6) is highly conserved. Since OAT from *Vigna* and 1OAT are well conserved in both sequence and structure, their biological function should be identical. The structure–structure comparison of template and the final refined models of OAT were performed using JOY program. It was noticed that the residues in the site 4, Tyr22, Leu46, Gly106, Val107, Phe141, Arg144, Glu194, Glu199, Asp227, Gln230, Lys256, Gly281 and Arg369 are conserved with the active site of template 1OAT (Fig. 5). The active site of 1OAT enzyme includes all the residues as mentioned above and among the twelve sites the shape of site 4 in OAT is similar to that of the catalytic site in 1OAT. Thus, in this study, site 4 was chosen as the most favorable binding site to dock the substrate and the inhibitors and the remaining 11 sites are therefore not discussed further. Thus, we suggest that inhibitors bind in a similar

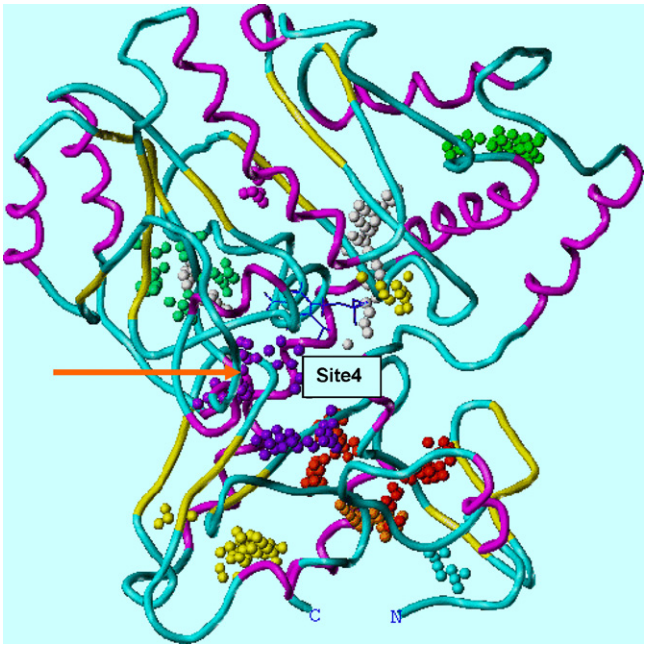

Fig. 6. The possible binding-sites of OAT model. Site 1 is represented by cyan, site 2 by red orange, site 3 by violet, site 4 by red, site 5 by green blue, site 6 by magenta, site 7 by yellow, site 8 by green, site 9 by white, site 10 by white, site 11 by purple and site 12 by orange color.

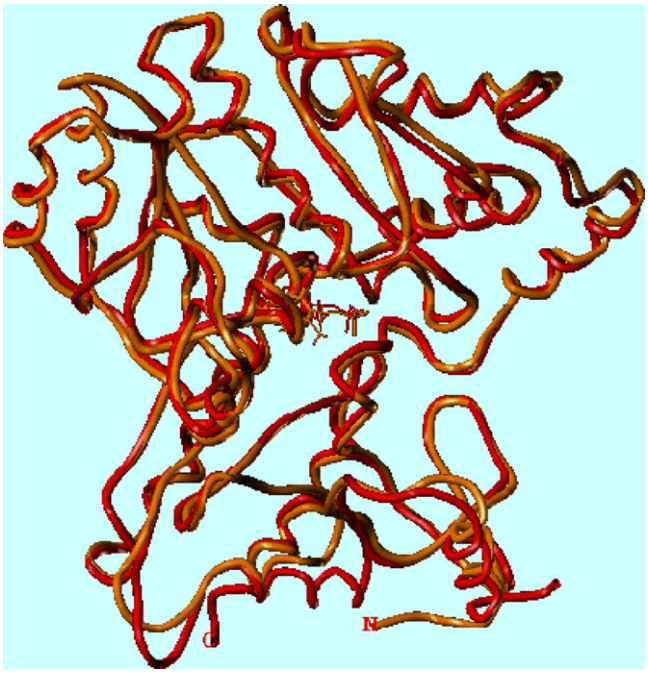

Fig. 7. Superimposition of Cα trace of OAT (represented in orange color) and 1OAT (represented in red color). N and C terminals are represented in blue colour.

manner for both the OAT enzyme and 1OAT. The final stable structure of OAT enzyme obtained is shown in Fig. 2.

3.7. Docking studies of OAT

Docking of the substrate with OAT was performed using GOLD, which was set to 50 cycles of run. Initially, protein–ligand complex was generated using GOLD package without constraints between the ligand and specific amino acids of the pocket. The algorithm exhaustively searches the entire rotational and translational space of the ligand with respect to the receptors. The flexibility of the ligand is given by dihedral angle variations. Various solutions evaluated by a score are equivalent to the absolute value of the total energy of the ligand in the protein environment. To understand the interaction between OAT enzyme, substrate and inhibitors, OAT-substrate and OAT-inhibitor complexes were generated using SYBYL software suite (Fig. 9). It is evident from the figure that substrate and inhibitors are located in the center of the active site and are stabilized by hydrogen bonding interactions. The hydrogen bonds present in enzyme-substrate and enzyme-inhibitor complexes along with their distances and angles are listed in Table 5. The binding of key residues in the active site of the model were determined based on the interaction energies of the substrate with residues in the active site of the enzyme. This identification, based on the distance from the substrate clearly showed the relative significance for every residue. Table 6 shows the interaction energies including the total, electrostatic and steric energies for all the residues in the active site of enzyme-substrate and enzyme-inhibitor complexes. It is evident from Table 6 that the enzyme-valine complex has large favorable total interaction energy of −5.075 kcal/mol. The electrostatic and steric energies for valine are −1.401 and −4.05 kcal/mol, respectively. These results indicate that both electrostatic and steric energies are vital for the protein-substrate complex interaction. The interaction analysis revealed that Gly106 and Lys256 are important anchoring residues for the substrate and are the main contributors to the substrate interaction. Though the interaction energy does not include the contribution from water or the extended enzyme structure, this preliminary data along with the list of hydrogen bond interactions between the enzyme and the active site residues clearly support that Gly106 and Lys256 are key residues in the binding of ligands.

4. Discussion

Proline plays an important role in the adaptation of plants to soil salinity, drought and temperature stresses. Proline is synthesized not only from glutamate but also from arginine/ornithine (derived from the L-acetyl-glutamate pathway) in higher plants [15]. Ornithine is converted to glutamic γ-semialdehyde in plants by δ-OAT unlike *E. coli* and gram-positive bacteria where α-aminotransferase catalyzes ornithine to P2C. This product is reduced to proline by P2C reductase. In plants, δ-OAT does not catalyze the reversible conversion of GSA to ornithine, but in animals this reaction is common [32]. Since proline acts as a reserve source of carbon, nitrogen and energy during recovery from stress [8] and shown to reduce enzyme denaturation caused due to temperature and NaCl stresses [13], regulation of ornithine pathway for proline production is important. Over-expression of an *Arabidopsis* δ-OAT gene in rice conferred both salt and drought stress tolerance [34]. The contribution of δ-OAT to proline

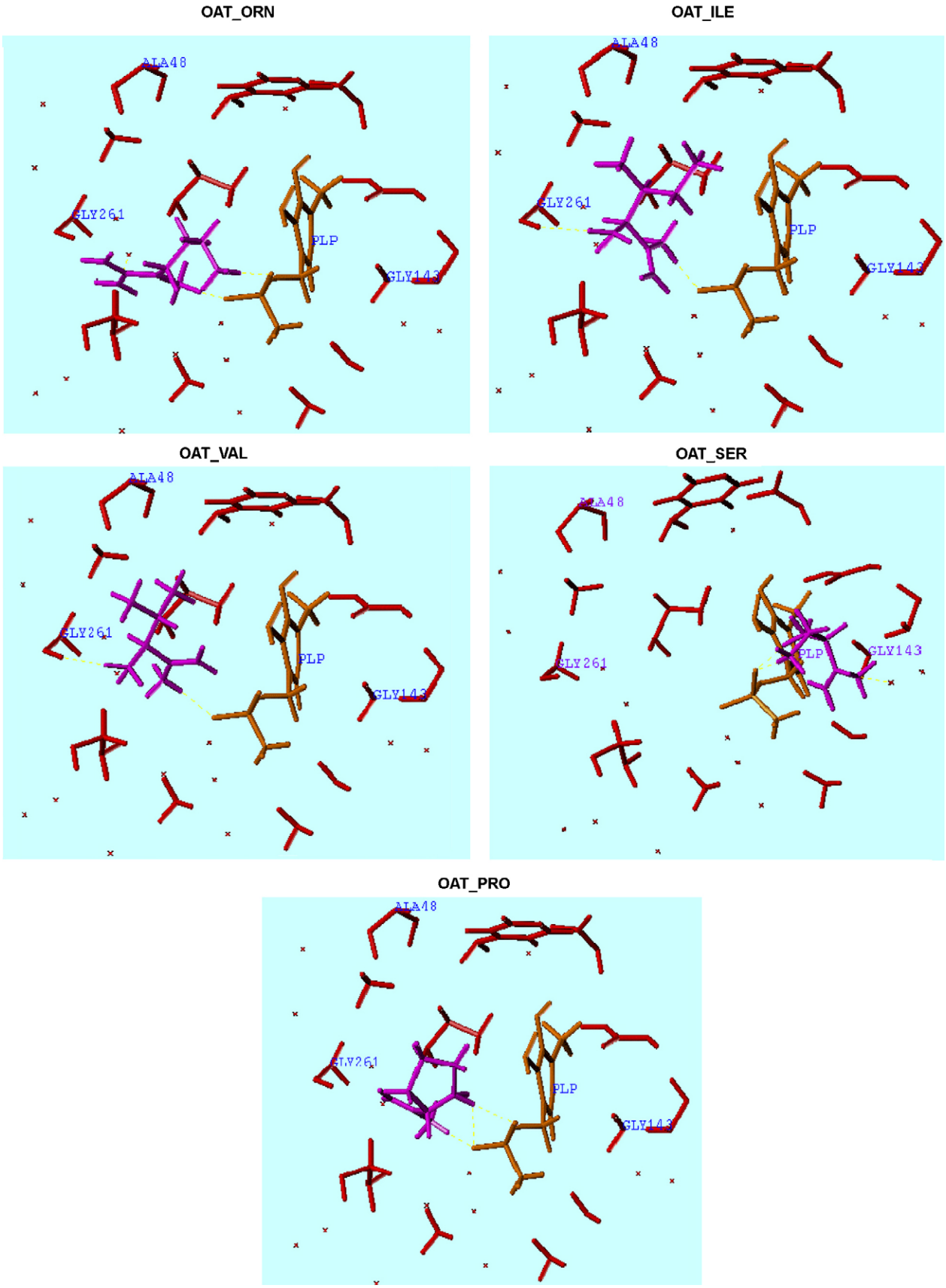

Fig. 8. Binding of inhibitors to OAT. Pyridoxal 5′-phosphate (cofactor) is represented in magenta and inhibitors are represented in blue color. Ornithine-OAT complex is represented as OAT_ORN; isoleucine-OAT complex as OAT_ILE; valine-OAT complex as OAT_VAL; serine-OAT complex as OAT_SER and proline-OAT as OAT_PRO.

biosynthesis during salt stress and following its withdrawal is not clear and its role is actively debated [10]. Though the relative contributions of glutamate and ornithine pathways for the production of proline (by estimating the transcript levels of P5CS and OAT) under salt stress were reported earlier [7,12], the activities of the respective enzymes were not reported under identical conditions. However, it was found in earlier studies of Delauney et al. [7] that the activity of OAT under salt stress was down-regulated unlike that of P5CS. They revealed that ornithine pathway is not predominant under NaCl stress conditions in *Vigna*. Wrench et al. [33] reported that ornithine is an important precursor for proline biosynthesis in Jerusalem artichoke (*Helianthus tuberosus*) and by contrast glutamate is the primary precursor for proline biosynthesis in osmotically stressed plants [23,24]. δ-OAT clone was isolated from *Arabidopsis* and its expression was studied during salt stress. Contrary to the results of Delauney et al. [7], an increase in both P5CS and OAT mRNA levels were reported under salt stress conditions in *Arabidopsis*. Since all these studies were carried out on different plant species that vary in age and developmental stage, the differences in OAT activity could be attributed to such conditions. Thus, both pathways appeared to be playing important roles under abiotic stress in plants. In the present study, the plant protein OAT was expressed in *E. coli*, partially purified and its activity was estimated in presence of different amino acids. In earlier studies with rat liver and kidney, PLP stimulated ornithine synthesis and OAT activity [9]. Omission of PLP reduced the specific activity of OAT by 60% in the present study, thus confirming the earlier studies carried in animals. The activity of the enzyme OAT is inhibited by isoleucine, valine and to some extent serine but not by proline. To further evaluate the effect of amino acids and their binding energies with the enzyme, *in silico* analysis was carried out by building a 3D model of OAT enzyme using the MODELLER6v2 software and subsequently a refined model was obtained after energy minimization methods. The final refined model was assessed by VERIFY-3D and PROCHECK programs and the results showed that this model is reliable. Therefore, this structure was subsequently used for docking of the ligands. Docking results indicated that conserved amino-acid residues Tyr22, Leu46, Gly106, Val107, Phe141, Arg144, Glu194, Glu199, Asp227, Gln230, Lys256, Ser266, Gly281 and Arg369 in OAT enzyme play an important role in maintaining a functional conformation and are directly involved in donor–substrate binding. Based on the interaction energies it was noticed that isoleucine and valine are the most preferred inhibitors and that there is a simple competitive inhibition between ornithine and valine which is consistent with the experimental data. Furthermore, Gly106 and Lys256 residues are involved in inhibitor binding and are conserved between the two enzymes (1OAT and OAT) and form hydrogen bonding with the inhibitors. It is known that hydrogen bonds play important role in the structure and function of biological molecules, especially for the catalysis. Valine has an interaction energy of −5.075 kcal/mol which is higher than the interaction energies of isoleucine (0.671 kcal/mol), serine (9.74 kcal/mol) and proline (1.650 kcal/mol). It was found that both ornithine and valine bound with the same atom, O1 (oxygen1) of PLP, the cofactor but they differed in binding site of Lys256. While the substrate ornithine bound to oxygen atom of Lys256, valine

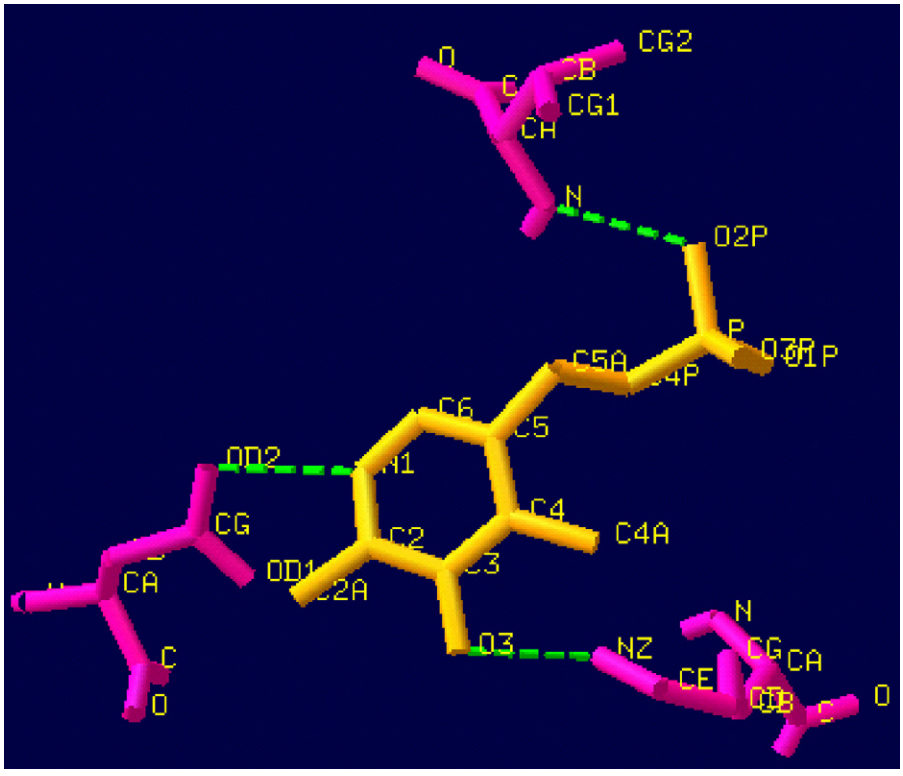

Fig. 9. Binding of PLP with the residues in the active site of OAT is predicted using SPDBV software suite.

Table 5
Hydrogen bonds along with their distances and angles between the substrate, inhibitors and active site residues of OAT as deciphered using SYBLY software suite

Ligand	Hydrogen Bonding		Distance	Angle
	Ligand atom	atom OAT		
Orn	ORN H2----------O1 PLP		1.337 A°	174.69°
(Substrate)	ORN H11---------O3PLP		2.068 A°	168.78°
	ORN H----------O LYS 256		1.761 A°	95.59°
	ORN H11---------O1PLP		2.729 A°	168.78°
Ile	ILE N----------O1PLP		1.533 A°	114.56°
	ILE O----------O3PLP		3.327 A°	172.92°
Val	VALHNCAP------O1 PLP		1.655 A°	168.81°
	VAL O----------H LYS256		2.487 A°	114.58°
Ser	SERHG--------- --O3P PLP		2.020 A°	166.39°
	SERHNCAP----- O3P PLP		1.651 A°	165.17°
	SERO----------H GLY 106		1.589 A°	156.47°
Pro	PROHNCAP----- O1PLP		2.549 A°	133.35°
	PROHOCAP---- O1 PLP		1.821 A°	170.32°
	PRO O----------H GLY106		1.971 A°	111.04°

Abbreviations—Orn: ornithine; Ile: isoleucine; Val: valine; Ser: serine; Pro: proline.

bound to hydrogen atom of Lys256. Oxygen, which contains one lone pair of electrons, is able to participate in electron transfer reactions. Ornithine, which contains delta amino group, is able to transfer its delta group because of its binding to oxygen atom of Lys256 and therefore can act as a substrate. Although valine is binding with the PLP cofactor at the same atom where ornithine is binding, because of differences in binding to Lys256 atom and lack of delta amino group, it was unable to participate in the reaction like that of ornithine. Hence, valine can act as a competitive inhibitor of ornithine but not as a substrate even though valine showed higher binding energy to the enzyme than ornithine. Isoleucine, which also inhibited the activity of OAT bound to O1 and O3 oxygen atoms of PLP cofactor but not to Lys256 where ornithine and valine were binding. Therefore, isoleucine showed lesser inhibition than valine. On the other hand, serine bound to O3 oxygen atom of PLP and hydrogen atom of Gly106 but showed lesser binding affinity than valine. Proline, which is an imino acid, contains a secondary amino group and hence it forms cyclic ring structure. The cyclic nature of proline is indeed unable to act as a competitive inhibitor to

Table 6
The total energy (E_{total}), electrostatic energy (E_{ele}), steric energy (E_{ste}) of the best-docked conformations

Substrate	E_{tota} (kcal/mol)	E_{ele} (kcal/mol)	E_{ste} (kcal/mol)
Orn	54.043	−13.331	67.374
Ile	0.671	−2.450	3.120
Val	−5.075	−1.401	−4.050
Ser	9.740	−1.082	10.823
Pro	1.650	−4.638	6.288

Substrate abbreviations are as described in Table 4.

ornithine. Proline bound to O1 of oxygen atom of PLP where ornithine and valine were binding but showed interactions with hydrogen of Gly106 instead of Lys256, which is an important residue in the binding of substrate and inhibitor. Probably because of this reason, proline also showed lesser inhibition on the activity of OAT than valine. Hence, proline cannot act as an inhibitor of the enzyme. Also, it was found that PLP, the cofactor of the enzyme bound with Val107, Asp227 and Lys256. In the presence of Schiff base, PLP interacts with Lys256 through a covalent bond formation, which is very important in converting the substrate to the product. Interactions of N1 of PLP with OD2 of Asp227 and O2P of PLP with nitrogen of Val107 are also very important for substrate and inhibitory activity (Fig. 8). Also, *in vitro* studies revealed that in presence of valine, specific activity of OAT was higher (5.3) than isoleucine (2.9). Based on these findings, it was predicted that valine is a preferred inhibitor with higher binding affinity than the other amino acids. When the activity of rat liver OAT was tested by branched-chain amino acids (L-valine-L-isoleucine-L-leucine), the inhibitory action was largely dependent on the branched structure of the hydrophobic residue where the carboxyl group was essential, but the α-amino group was only complementary [30]. The kinetic results showed that L-valine interacts with the phosphopyridoxal enzyme, resulting in the inhibition of the forward reaction, but valine is a non-competitive inhibitor in the reverse reaction. Both α and δ-amino exchange as well as the overall reactions were affected by L-valine [29]. The interactions between the enzyme and the inhibitors proposed in this study are useful for understanding the potential mechanism of enzyme and substrate binding. These findings thus corroborate the results obtained *in vitro*. However, it is important to see how the activity of δ-OAT varies as a function of plant development during salt stress vis-à-vis the proline synthesis.

Acknowledgements

The authors are thankful to the Director, Center for Distance Education, Osmania University, for his kind support, cooperation and also for providing the bioinformatics facilities. We are thankful to the CSIR, New Delhi, for financial assistance in the form of a research project.

References

[1] B.J. Alder, T.E. Wainwright, Studies in molecular dynamics. I. General methods, J. Chem. Phys. 31 (1959) 459–466.

[2] S.F. Altschul, W. Gish, W. Miller, E.W. Myers, D.J. Lipman, Basic local alignment search tool, J. Mol. Biol. 215 (1990) 403–410.
[3] S.F. Altschul, T.L. Madden, A.A. Schaffer, J. Zhang, Z. Zhang, W. Miller, D.J. Lipman, Gapped BLAST and PSI-BLAST: a new generation of protein database search programs, Nucleic Acids Res. 50 (1997) 3389–3402.
[4] M.M. Bradford, A rapid and sensitive method for quantitation of microgram quantities of protein utilizing the principle of protein–dye binding, Anal. Biochem. 72 (1976) 248–254.
[5] A.J. Delauney, D.P.S. Verma, A soybean gene encoding Δ^1-pyrroline-5-carboxylate reductase was isolated by functional complementation in *Escherichia coli* and is found to be osmoregulated, Mol. Gen. Genet. 221 (1990) 299–305.
[6] A.J. Delauney, D.P.S. Verma, Proline biosynthesis and osmoregulation in plants, Plant J. 4 (1993) (1993) 215–223.
[7] A.J. Delauney, C.-A.A. Hu, P.B. Kavi Kishor, D.P.S. Verma, Cloning of ornithine δ-aminotransferase cDNA from *Vigna aconitifolia* by transcomplementation in *Escherichia coli* and regulation of proline biosynthesis, J. Biol. Chem. 268 (1993) 18673–18678.
[8] P.D. Hare, W.A. Cress, Tissue specific accumulation of transcript encoding Δ^1-pyrroline-5-carboxylate reductase in *Arabidopsis thaliana*, Plant Growth Reg. 19 (1996) 249–256.
[9] J.G. Hensless, M.E. Jones, Ornithine synthesis from glutamate in rat small intestinal mucosa, Arch. Biochem. Biophys. 219 (1982) 186–197.
[10] F. Hervieu, L. Le Dily, C. Huault, J.P. Billard, Contribution of ornithine δ-aminotransferase to proline accumulation in NaCl-treated radish cotyledons, Plant Cell Environ. 18 (1995) 205–210.
[11] C.M. Ho, G.R. Marshall, Cavity search: an algorithm for isolation and display of cavity-like binding regions, J. Comput. Aided Mol. Des. 4 (1990) 337–354.
[12] C-A.A. Hu, A.J. Delauney, D.P.S. Verma, A bifunctional enzyme (Δ^1-pyrroline-5- carboxylate synthetase) catalyzes the first two steps in proline biosynthesis in plants, Proc. Natl. Acad. Sci. U.S.A. 89 (1992) 9354–9358.
[13] S. Iyer, A. Caplan, Products of proline catabolism can induce osmotically regulated genes in rice, Plant Physiol. 116 (1998) 203–211.
[14] G. Jones, P. Willett, R.C. Glen, A.R. Leach, R. Taylor, Development and validation of a genetic algorithm for flexible docking, J. Mol. Biol. 267 (1997) 727–748.
[15] P.B. Kavi Kishor, S. Sangam, R.N. Amrutha, P. Sri Laxmi, K.R. Naidu, K.R.S.S. Rao, K.J. Sreenath Rao, P. Reddy, N. Theriappan, Sreenivasulu, Regulation of proline biosynthesis, degradation, uptake and transport in higher plants: its implications in plant growth and abiotic stress tolerance, Curr. Sci. 88 (2005) 424–438.
[16] R.A. Laskoswki, M.W. MacArthur, D.S. Moss, J.M. Thornton, PROCHECK: a program to check the stereo chemical quality of protein structures, J. Appl. Cryst. 26 (1993) 283–291.
[17] R. Lüthy, J.U. Bowie, D. Eisenberg, Assessment of protein models with three-dimensional profiles, Nature 356 (1992) 83–85.
[18] T. Maniatis, E.F. Fritsch, I. Sambrook, Molecular Cloning: a Laboratory Manual, Cold Spring Harbor Laboratory Press, Cold Spring Harbor, NY, 1982.
[19] K. Mizuguchi, C.M. Deane, T.L. Blundell, M.S. Johnson, J.P. Overington, JOY: protein sequence-structure representation and analysis, Bioinformatics 14 (1998) 617–623.
[20] S.B. Needleman, C.D. Wunsch, A general method applicable to the search for similarities in the amino acid sequence of two proteins, J. Mol. Biol. 48 (1970) 443–453.
[21] M.J.D. Powell, Restart procedures for the conjugate gradient method, Math. Program. 12 (1977) 241–254.
[22] W.H. Press, B.P. Flannery, S.A. Teukolsky, W.T. Vetterling, Numerical Recipes in C, The Art of Scientific Computing, Cambridge University Press, U.K., 1998.
[23] D. Rhodes, S. Handa, R.A. Bressan, Metabolic changes associated with adaptation of plant cells to water stress, Plant Physiol. 82 (1986) 890–903.
[24] N.H.C.J. Roosens, T.T. Thu, H.M. Iskandar, M. Jacobs, Isolation of ornithine-δ-aminotransferase cDNA and effect of salt stress on its expression in *Arabidopsis thaliana*, Plant Physiol. 117 (1998) 263–271.
[25] A. Sali, T.L. Blundell, Comparative protein modeling by satisfaction of spatial restraints, J Mol. Biol. 234 (1993) 779–815.
[26] S.A. Shah, B.W. Shen, A.T. Brunger, Human ornithine aminotransferase complexed with L-canaline and gabaculine: structural basis for substrate recognition, Structure 5 (1997) 1067–1075.
[27] B.W. Shen, M. Hennig, E. Hohenester, J.N. Jansonius, T. Schirmer, Crystal structure of human recombinant ornithine aminotransferase, J. Mol. Biol. 277 (1998) 81–102.
[28] C.R. Stewart, Proline accumulation: biochemical aspects, in: L.G. Paleg, D. Aspinall (Eds.), The Physiology and Biochemistry of Drought Resistance in Plants, Academic Press, Sydney, 1981, , pp. 243–258, ISBN: 0-12-544380-3.
[29] P. Storici, G. Capitani, R. Müller, T. Schirmer, J.N. Jansonius, Crystal structure of human ornithine aminotransferase complexed with the highly specific and potent inhibitor 5-fluoromethylornithine, J. Mol. Biol. 285 (1999) 297–309.
[30] T. Matsuzawa, Characteristics of the inhibition of ornithine-δ-aminotransferase by branched-chain amino acids, J. Biochem. 75 (3) (1974) 601–609.
[31] J.D. Thompson, D.G. Higgins, T.J. Gibson, CLUSTAL W: improving the sensitivity of progressive multiple sequence alignment through sequence weighting, position-specific gap penalties and weight matrix choice, Nucleic Acids Res. 22 (1994) 4673–4680.
[32] D. Voet, J.G. Voet, Biochemistry, 2nd ed., John Wily and Sons Publication, New York, USA, 1990, ISBN 0-471-58651.
[33] P. Wrench, C.J. Brady, R.W. Hinde, Interaction of slicing and osmotic stress on proline metabolism in Jerusalem artichoke tuber tissue, Aust. J. Plant Physiol. 7 (1980) 149–157.
[34] L.Q. Wu, Z.M. Fan, L. Guo, Y.Q. Li, W.J. Zhang, L.J. Qu, Z.L. Chen, Over-expression of an *Arabidopsis* δ-OAT gene enhances salt and drought tolerance in transgenic rice, Chin. Sci. Bull. 48 (2003) 2594–2600.